

Determination of Corrosion Types from Electrochemical Noise by Artificial Neural Networks

Li Jian^{1,*}, Kong Weikang¹, Shi Jiangbo², Wang Ke², Wang Weikui¹, Zhao Weipu¹, Zeng Zhoumo¹

¹ State Key Laboratory of Precision Measuring Technology and Instrument, Tianjin University, Tianjin 300072, P.R. China

² School of Materials Science and Engineering, Tianjin University, Tianjin 300072, P. R. China

*E-mail: tjupipe@tju.edu.cn

Received: 20 December 2012 / Accepted: 13 January 2013 / Published: 1 February 2013

In this paper, a novel approach for distinguishing the type of corrosion from Electrochemical Noise (EN) signals is presented. A database containing numerous sets of original EN data is established, then the database is divided into training sets and test sets randomly. The EN data sets are used as the inputs of the Artificial Neural Networks (ANN) and the types of corrosion as the outputs of the ANN. A feature vector is extracted from each EN data set. Subsequently, two kinds of artificial neural networks with different neural structures, the Back Propagation (BP) and the Support Vector Machine (SVM), are constructed by training feature vector. The test sets are used to test the accuracy of the two neural networks. The result shows the ANN is a very accurate and effective way to distinguish the type of corrosion and the SVM is more accurate than the BP.

Keywords: Electrochemical Noise; Artificial Neural Networks; Feature vector; Back Propagation (BP); Support Vector Machine (SVM)

1. INTRODUCTION

1.1 Electrochemical noise

304 stainless steel is widely used in the field of engineering due to its good performance in corrosion resistance and mechanical properties. [1-3]. The corrosion behaviors of it under different working conditions have been studied using different techniques such as X-ray photoelectron spectroscopy (XPS)[4], photoelectrochemical method[5], scanning Kelvin probe (SKP)[5], dynamic electrochemical impedance spectroscopy (DEIS)[6, 7], scanning electron microscope (SEM), and acoustic emission (AE) [2, 8-12].

Electrochemical noise (EN) is defined as the fluctuations of potential and current generated spontaneously during the corrosion processes [14, 15]. The EN originates from the random ion movements in the electrolyte/electrode interface [13]. Unlike the traditional electrochemical techniques (potentiodynamic polarization tests, impedance spectroscopy, etc), EN measurements can be performed in freely corroding systems without the external application of electrical signals, so that the natural evolution of corrosion processes is assured [17].

Recently, the focus of studies on EN is the electrochemical noise analysis (ENA). The original EN data usually appears to be complicated. How to extract meaningful parameters, which characterize the corrosion process, is the difficulty of research. Many methods such as Electrochemical Noise Resistance (R_n) in time domain [4, 14, 15], the Fast Fourier Transform (FFT) in frequency domain [20, 21], the average charge in each event (q) and the frequency of events (f_n) derived from shot noise theory [16], the energy distribution (ED) from wavelet transform [17, 18], fractal geometry [25, 26], the correlation dimensions by the phase space methods [27-29] etc have been proposed.

Artificial neural network is a new approach to differentiate corrosion types. Although ANN has been developed extensively over many years, especially in the field of forecast, fitting, pattern recognition, few people apply it to the research of electrochemical noise. The ANN use multi-parameters to distinguish corrosion types jointly instead of using one parameter independently. There is no need to establish the evaluation mathematical model of various parameters or identify the weights of each parameter. Moreover, ANN is a kind of machine learning which can substitute for human brain to complete recognition. Furthermore, it can be used in real-time systems due to the high processing speed.

In this paper, ANN with the ability to learn from experimental values is used as an intelligent information processing system to distinguish the corrosion types. This process can be seen as an application of pattern recognition. The ANN learned from training data and recognized different corrosion types from a series of input (feature vectors containing many parameters) and output (different corrosion types) without any prior assumptions about their nature and interrelations [30]. Therefore, ANN could be a useful tool in determining the corrosion types from electrochemical noise.

1.2 Artificial Neural Networks

The artificial neural network is a mathematical model of simulating human neurons to process information. It can be used to do pattern recognition, fitting (when it can't be expressed using a formula or the formula is complicated) and forecasting etc.

In this paper, BP neural network and SVM are designed. A typical BP neural network structure is showed in fig 1. In order to design a BP ANN three parameters must be determined: the number of nodes, the learning rate and the learning function. The number of nodes affects the ANN accuracy: less nodes lead to lower accuracy and relatively shorter training times, while more nodes lead to over-fitting and longer training time. The learning rate is the speed of weight update. The larger the learning rate, the faster the network will learn. However it will cause a weight shock which must be avoided. The learning function is the function used in hidden layer, which can affect the ANNs' accuracy and

efficiency. Choosing three appropriate parameters which lead to the highest accuracy is significant for designing a BP ANN.

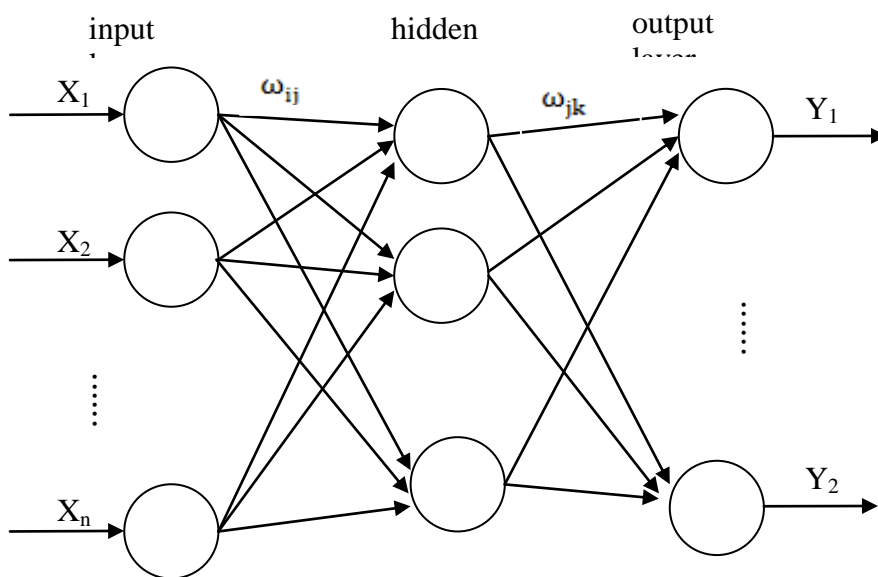


Figure 1. The architecture of the BP ANN model.

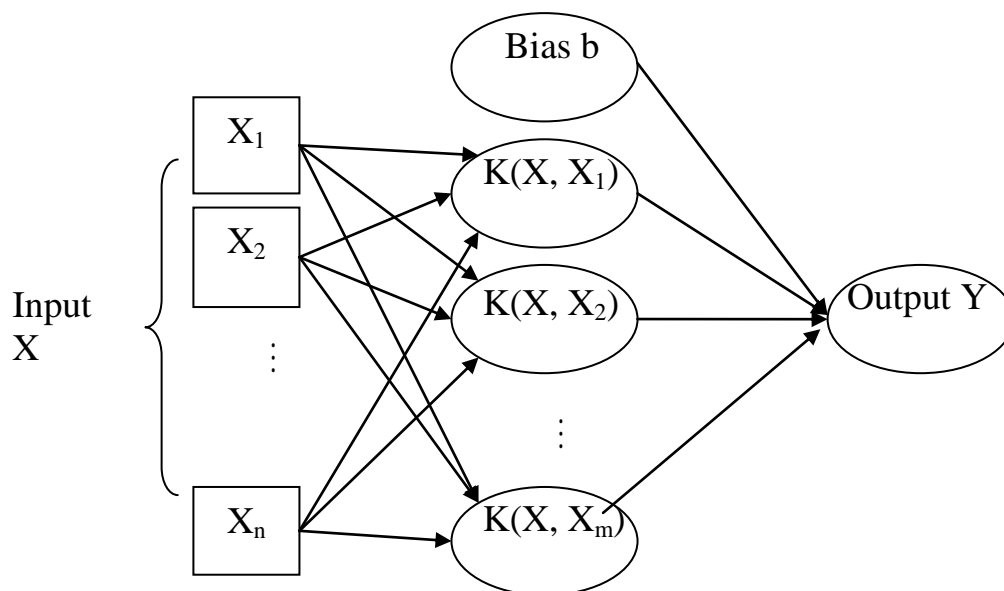


Figure 2. SVM architecture

The SVM is a new kind of learning machine that uses the central concept named kernel for a number of learning tasks. Kernel machines provide a modular framework that can be adapted to different tasks and domains by using different kernel function (i.e., linear, polynomial, sigmoid or radial basis) and the base algorithm. SVMs have good performance in solving classification and

regression problems. The principle of classification, achieved by method of neural networks, is to find an optimal hyperplane to maximize the edge between Positive examples and the counter examples [31-33].

The support vector machine architecture is shown in fig 2, where k is the kernel function, such as:

$$\text{linear : } K(\mathbf{x}, \mathbf{x}_i) = \mathbf{x}^T \mathbf{x}_i \quad (1)$$

$$\text{polynomial: } K(\mathbf{x}, \mathbf{x}_i) = (\gamma \mathbf{x}^T \mathbf{x}_i + r)^p, \gamma > 0 \quad (2)$$

$$\text{radial basis: } K(\mathbf{x}, \mathbf{x}_i) = e^{(-\gamma \|\mathbf{x} - \mathbf{x}_i\|)}, \gamma > 0 \quad (3)$$

$$\text{sigmoid: } K(\mathbf{x}, \mathbf{x}_i) = \tanh(\gamma \mathbf{x}^T \mathbf{x}_i + r) \quad (4)$$

Design a SVM requires determine three parameters: the cost (c), the gamma (γ) and the kernel function (t). The cost is error tolerance. The higher the value, the more networks can't tolerate errors. The gamma relates to the kernel function, like the γ in the formula (4); the kernel function is the function selected. The optimal parameters that lead to the highest accuracy are obtained by various optimization algorithms. The optimization algorithms usually used are cross validation (K-CV), genetic algorithm (GA) and particle swarm optimization (PSO).

2. EXPERIMENTAL

2.1 Specimens preparation

The specimen used in this study was 304 stainless steel (SS) (chemical composition, in mass fraction, %: C \leq 0.080%; Cr 18.0%-20.0%; Ni 8.00%-11.0%; Mn \leq 2.0%; Si \leq 1.0%; P, \leq 0.045%; S \leq 0.03%; Fe, balance). From the SS plates, 10mm \times 10mm \times t mm (thickness) specimens were cut, then the specimens were mounted in epoxy with only the working electrode surface of 1cm² exposed. The exposed surface was grinded using abrasive papers through 500-grade to 3000-grade, polished with diamond paste, rinsed using acetone, degreased with deionized water and dried in air. A saturated calomel electrode (SCE), with a salt bridge, was used as a reference electrode (RE).

2.2 Experimental conditions

A three-electrode setup was used for the experiments. Two nominally identical WEs were immersed in the selected solutions. The potential and current were measured simultaneously through a zero resistance ammeter (ZRA) mode via a data acquisition system working as a multi-channel electrochemical workstation. This system is constructed by NI-CRIO and developed software.

The electrolytes used in this experiment were summarized in Table 1, and the corresponding corrosion type was inferred from visual observation of the sample, coupled with the behavior of these systems as reported by earlier workers and visual interpretation of the electrochemical noise time records. All experiments were under the room temperature ($25^{\circ}\text{C} \pm 3^{\circ}\text{C}$). The data processing and neural network were implemented by Matlab2011.

Table 1. Experimental solutions

experiment	Solutions	Corrosion type	Duration (h)	Label
1	0.1mol/l FeCl ₃	Pitting	72	PT1
1	0.2mol/l FeCl ₃	Pitting	72	PT2
1	0.3mol/l FeCl ₃	Pitting	72	PT3
2	0.5mol/l H ₂ SO ₄	Uniform corrosion	72	U1
2	0.6mol/l H ₂ SO ₄	Uniform corrosion	72	U2
2	0.7mol/l H ₂ SO ₄	Uniform corrosion	72	U3
3	0.1mol/l NaOH +0.1mol/l KOH	Passivation	72	P1

3. DEVELOPMENT OF THE ARTIFICIAL NEURAL NETWORKS

During the experiment, both the current between the two working electrodes and the potential of the SS specimens against an SCE are simultaneously recorded for 72 hours. These records are analysed for each solution. The flow chart shows the data analysis procedure by ANN(fig 3).

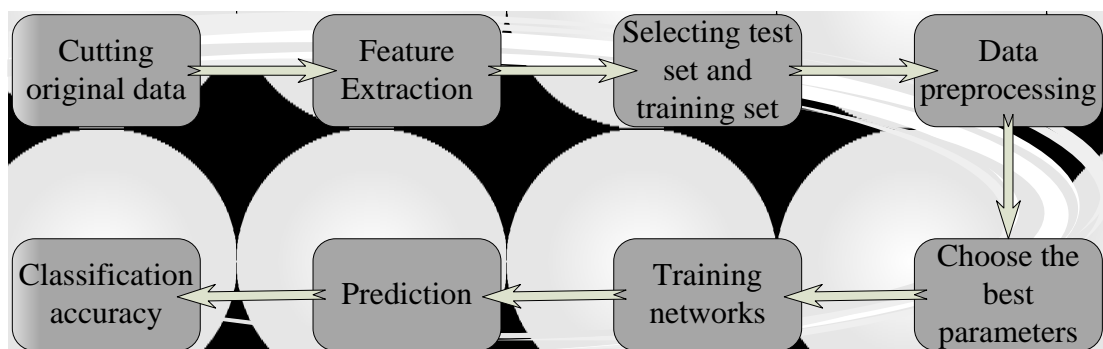


Figure 3. The flow chart of the development of ANN

The sampling interval in experiment is 0.5s and each data record consisted of 1024 datapoints(512s), from which a feature vector is extracted. In this paper, a feature vector contained 10 elements: R_n , q , f_n , the energy of 7-level wavelet crystal. The formula is listed as follows:

$$R_n = \sigma_E / \sigma_I \quad (5)$$

q and fn:

$$I_{corr} = qf_n \quad (6)$$

$$f_n = \frac{I_{corr}}{q} = \frac{B^2}{\psi_E} \quad (7)$$

$$q = \frac{\sqrt{\psi_E \psi_I}}{B} \quad (8)$$

EDP:

$$E_j^d = \frac{1}{E} \sum_{k=1}^{N/2^j} d_{j,k}^2 \quad (9)$$

$$E_j^s = \frac{1}{E} \sum_{k=1}^{N/2^j} s_{j,k}^2 \quad (10)$$

$$E = E_j^d + E_j^s \quad (11)$$

Where, σ_E, σ_I are the standard deviation of potential and current after removal of DC; ψ_E, ψ_I are the low frequency PSD values of the potential and current noise respectively; B is the Stern–Geary coefficient ; $d_{j,k}, s_{j,k}$ are the coefficient decomposed by Daubechies-4 wavelet to seven levels, j stands for the level.

After the above data process, the original data have been converted to numerous feature vectors. Then 100 feature vectors are selected randomly from three kinds of corrosion as input signals. Among these 100 feature vectors, 80% (80) of them are selected as training sets and the rest 20% (20) as the test sets. Before training the ANN model, both input and output variables should be normalized within the range from 0 to 1 in order to eliminate the gap between each feature value to improve the accuracy. The typical normalized function is shown as follow:

$$X_k = (X_k - X_{min}) / (X_{max} - X_{min}) \quad (12)$$

Where X_{min} and X_{max} are the maximum and the minimum value. After this, cross validation (K-CV) is selected to find the best c, g in SVM. A validation set is selected to find the best learning rate and learning function in BP ANN. Training sets are used to train the network, then, this trained network is been used to predict the type of the test set. The prediction accuracy is achieved as follow:

$$accuracy = N_c / N \quad (13)$$

where N_c is the number of the correct prediction and N is the total number of the test set. Accuracy is the most important parameter to evaluate the ANN.

4. RESULTS AND DISCUSSION

4.1. Preparing for training networks

A visual examination of the EN signals in the time domain exhibited certain typical features. The time records for all the potential and current noise records presented are trend removed by wavelet transform reference to [34], so as to eliminate the DC drift[35].

As references [27,36] have shown, the EN data of pitting will have some peaks, while the EN data of uniform corrosion and passivation appear frequent and irregular oscillation. Fig 4-a and 4-d show the potential and current records for AISI type 304ss in 0.2mol/l FeCl_3 after 2 hours of immersion. Well-defined peaks are observed in the current and potential noise record with high amplitude of 3mV and $7\mu\text{A}$, respectively. Visual examination of the surface after immersion show well-developed pits. Figure4-b and 4-e show records for 304ss in 0.6mol/l H_2SO_4 after 6 hours of immersion[37]. oth the current and potential noise oscillate frequently and irregularly within amplitude of 0.4mV and 200nA. The surface of the specimens becomes rough and grayed by sight. Figure4-c and 4-f show records for 304ss in 0.1mol/l NaOH + 0.1mol/l KOH after 2 hours of immersion. The noise records show similarity to those of the uniform corrosion, but the amplitude within 0.5mV and 0.5nA is significantly less and the oscillation frequency is also lower than the uniform corrosion. The surface shows no visible changes.

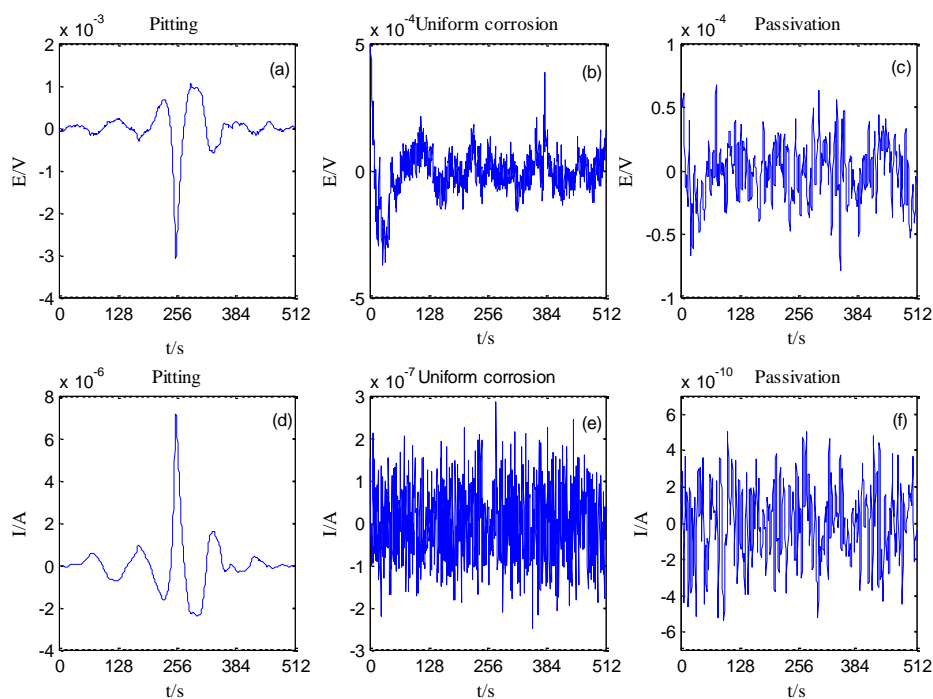


Figure 4. three kinds of EN data for pitting(a,d), uniform corrosion(b,e) and passivation(c,f).

As designed, a feature vector that consists of 10 elements is extracted from a set of 1024 data points. Fig 5 shows feature vector of 300 samples. The type plot (fig 5-a) shows that each corrosion

type contains 100 samples. As cottis et al[18,38] shows that the passivation have largest RN value larger than $10^5\Omega$, while uniform corrosion and pitting have smaller value of RN. The Rn plot (fig 5-b) shows an obvious gap between the value Rn of the passivation is larger with the value of $10^5\Omega$ while Rn of the other two is less than $10^4\Omega$. The q plot (fig 5-c) shows pitting has a large value of q compared with the other two corrosion types, because according to reference [22] q is a function of the tendency to localization. Fig5-e to k shows the energy distribution plot for different corrosion types. It shows that the relative energy distributions exhibit different features. For the pitting, the maximum is observed in the crystal d7, while for uniform corrosion the energy is mainly centred among the crystal d1-d3. As for passivation, the main energy distribution is among crystal d3-d5. Inferred from the theory of Wavelet decomposition, a large coefficient indicates a high similarity to the mother wavelet. So a peak leads to a large coefficient of large scale mother wavelet, in a similar way, high repetition rate leads to a large coefficient of small scale mother wavelet [23]. In conclusion, the performance in fig 5 is consistent with the results in fig 4 and the Wavelet decomposition theory.

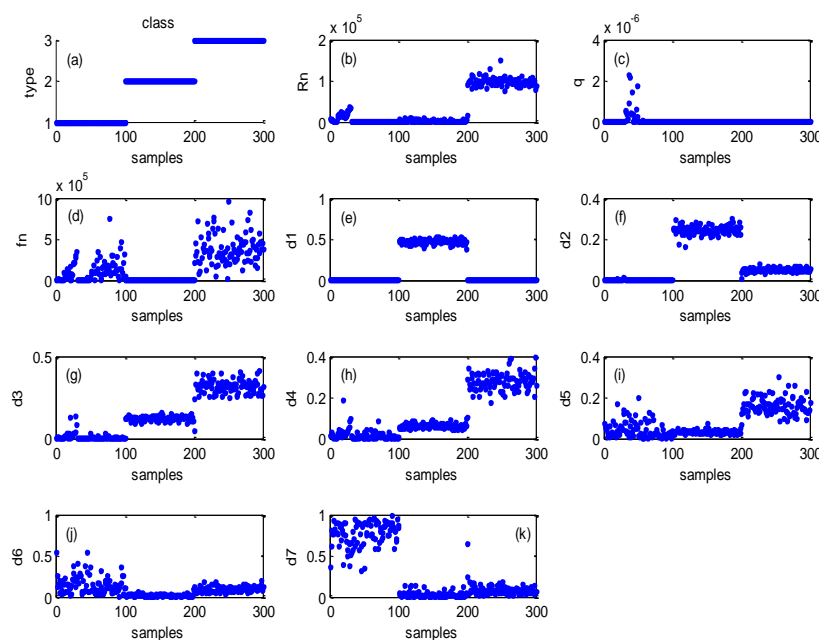


Figure 5. ten elements of 600 feature vectors

4.2 Result of BP

Before training BP neural networks, the number of hidden layers has to be determined. The input has 10 elements, so 9 hidden layers is suitable. The training function provided by matlab is used to train networks [39]. The training performance is shown in fig 6. The mean squared error (mse) reduces with iteration. At the beginning, the mse has a high convergence rate and the minimum value of validation mse (green lion) appears at epoch 26 (indicating iteration times). After then, more iteration times lead to the rise of mse. So the training stop at epoch 26 with the best validation mse value of 2.1381×10^{-6} .

The accuracy of the neural network is showed by the method as matrix in fig 7. The column of matrices is the output class and the row is the target class. The diagonal of matrix (in green) indicates the output class is the same as the target class. Similarly, the elements which are not on the diagonal (in red) indicates the wrong output. The grey boxes are the accuracy of each corrosion type, and the blue box is the accuracy of each set. There are 4 matrices corresponding to train set, validation set and all sets in fig 7. We can only find one wrong output in test matrix in fig 7, where the actual type is the 2nd class (uniform corrosion), but misclassified as 1st class(pitting). Obviously, the accuracy of the bp ANN is 99.7%(299/300).

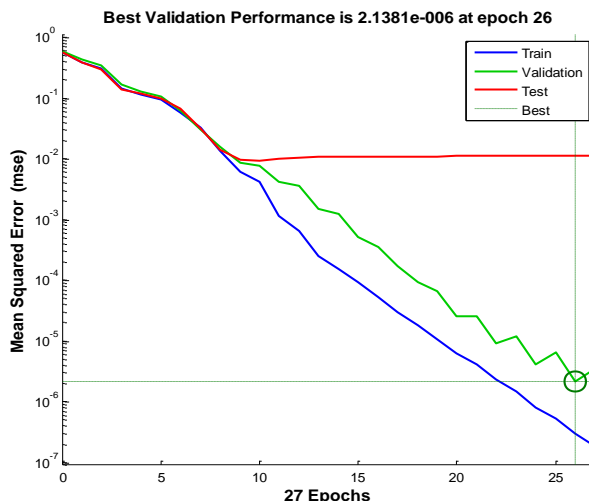


Figure 6. the training performance



Figure 7. the confusion matrix

4.3. Result of SVM

SVM is different from BP. It uses cross validation to find the best c and g . Cross validation is carried out by the following steps. The original training data is divided into k sets (Generally by average). Each set would be selected as a validation set, and the rest $k-1$ sets as the training set. Thus we got k models, and the CVAccuracy is the average accuracy of the k models [40,41].

The parameter selection results are showed by the gridsearch method in large step and small step in fig 8. After an approximate range of c and g is achieved in large step, an optimal value of c and g can be obtained in small step, maximizing the CVAccuracy. In fig 8, the x, y axis is log to log scale by the base of 2, and the z axis is CVaccuracy. A 3D view can help us find the best c and g in an intuitive observation. Fig 8 shows the best c is 0.25, and the best g is 0.0625 with the accuracy of 99.5833%.

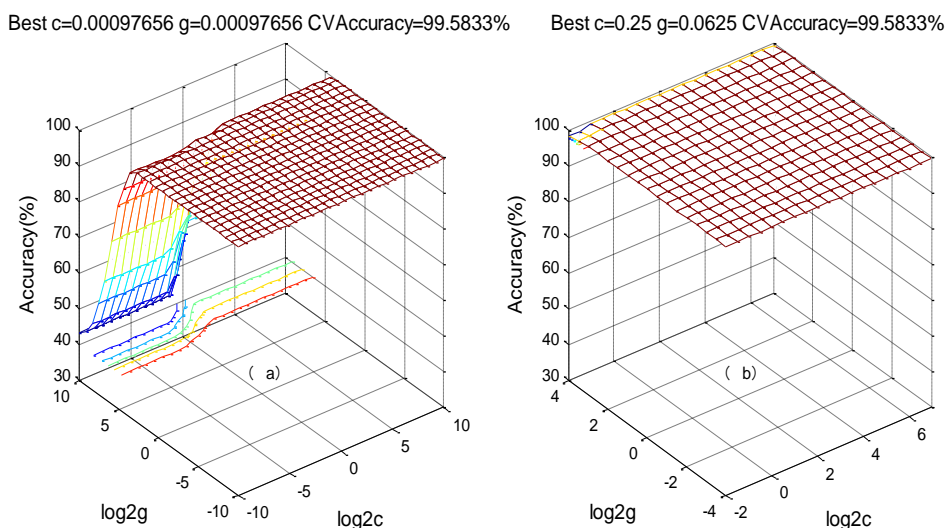


Figure 8. the parameter selection result by the gridsearch method in large step (a) and small step (b)

After locating the best c and g , the next step is applying them for training. Then the network is trained to predict the classification using the test set. Fig 10 shows the actual and predicted classification of the test set. In fig 10 actual type is represented by 'o', and the predicted type by SVM is represented by '*'. The predicted type is correct where 'o' coincides with '*'. The accuracy is exactly 100% (120/120) [31-33].

Furthermore, Fig 11 shows different results of typical morphology analysis of 304 SS after 72 hours of immersion. Original sample shows a smooth surface (in Fig 11-a). Well-developed pits are observed on the surface in solution PT1, PT2, PT3 (in Fig 11-b). Uniform corrosion shows that a serious general corrosion occurs on the surface in solution U1, U2, U3 (in Fig 11-c). Passivation shows the formation of a passive film that little corrosion occurs on the surface in solution p1 (in Fig 11-c).

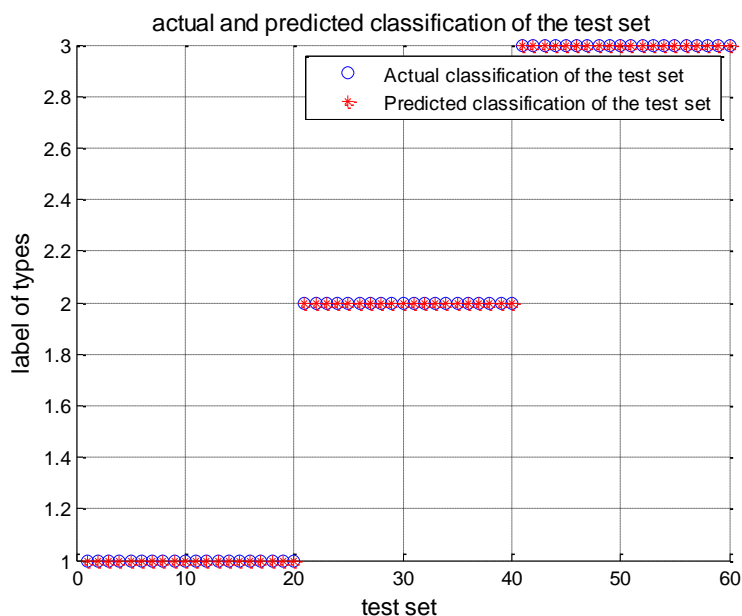


Figure 10. the actual and predicted classification of the test set

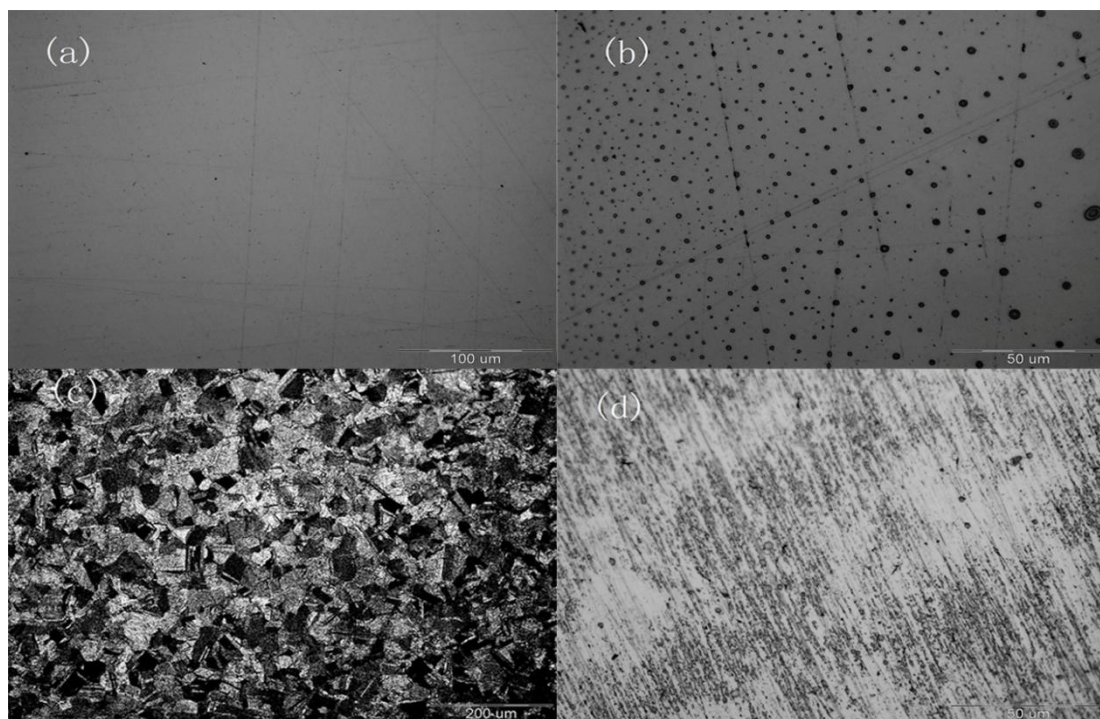


Figure 11. metallographical image of original sample (a), pitting (b), uniform corrosion (c) and passivation(d)

On all accounts, all the results obtained above obviously indicate that the well-trained ANN model ,whether BP or SVM, showed a good performance, with the accuracy of 99.7% and100%, on determination of corrosion types from electrochemical noise. An ANN is just like a black-box, the

internal structure of which is insignificant. Using matlab to package all function into an entire program can determinate the corrosion type from original EN data automatically and accurately.

5. CONCLUSIONS

In this paper, methods of artificial neural networks are employed to determinate corrosion types from electrochemical noise. A database is established to manage the data, which makes subsequent steps more convenient and efficient. After that, a reference EN data processing flow is proposed to develop the artificial neural networks. The neural network is optimized by the algorithm named cross validation (K-CV). Finally, the results show that BP has an accuracy of 99.7% and SVM has an accuracy of 100%, which evidently indicate that ANN has a high accuracy on distinguish the corrosion type. In conclusion, ANN is a novel effective and accurate methodology to process electrochemical noise and determinate the corrosion type.

ACKNOWLEDGEMENTS

The project was supported by the National Program on Key Basic Research Project (973 Program) (2011CB610505) and National Natural Science Foundation of China (61240038).

References

1. G. Du, J. Li, W.K. Wang, C. Jiang, S.Z. Song, *Corrosion Science* 53 (2011) 2918-2926.
2. R. Zhao, Z. Zhang, J.B. Shi, L. Tao, S.Z. Song, *Journal of Central South University of Technology* 17 (2010) 13-18.
3. A. Machet, A. Galtayries, S. Zanna, L. Klein, V. Maurice, P. Jolivet, M. Foucault, P. Combrade, P. Scott, P. Marcus, *Electrochimica Acta* 49 (2004) 3957-3964.
4. J.F. Chen, W.F. Bogaerts, *Corrosion Science* 37 (1995) 1839-1842.
5. Shenghan Zhang, Yu tan, *Journal of Nuclear Materials*, DOI :10.1016/j.jnucmat.2012.11.024
6. L.T. Han, F. Mansfeld, *Corrosion Science* 39 (1997) 199-202.
7. K. Darowicki, S. Krakowiak, P. Slepski, *Electrochimica Acta* 49 (2004) 2909-2918.
8. K. Darowicki, P. Slepski, M. Szocinski, *Progress in Organic Coatings* 52 (2005) 306-310.
9. G. Du, W.K. Wang, S.Z. Song, S.J. Jin, *Anti-Corrosion Methods and Materials* 57 (2010) 126-132.
10. J.A. Xu, X.Q. Wu, E.H. Han, *Corrosion Science* 53 (2011) 1537-1546.
11. A. Arutunow, K. Darowicki, *Electrochimica Acta* 53 (2008) 4387-4395.
12. A. Arutunow, K. Darowicki, *Electrochimica Acta* 54 (2009) 1034-1041.
13. W. Kuang, X. Wu, E.-H. Han, *Corrosion Science* 52 (2010) 4081-4087.
14. K. Hladky, J.L. Dawson, *Corros. Sci.* 22 (1982) 231.
15. R.A. Cottis, *Corrosion*. 57 (2001) 265-285.
16. R.A. Cottis, *Russian Journal of Electrochemistry* 42 (2006) 497-505.
17. E. Garcia-Ochoa, F. Corvo, *Electrochem. Commun.* 12 (2010) 826-830.
18. H.A.A. Al-Mazeedi, R.A. Cottis, *Electrochimica Acta* 49 (2004) 2787-2793.
19. U. Bertocci, C. Gabrielli, F. Huet, M. Keddam, *Journal of the Electrochemical Society* 144 (1997) 31-37.
20. Jurchustu, Dawson J L. *Corrosion*, 1987, 43 (1) : 19
21. Hldky K, Dawson J L. *Corros. Sci.* , 1982, 22 (3) : 231
22. J.M. Sanchez-Amaya, R.A. Cottis, F.J. Botana, *Corrosion Science* 47 (2005) 3280-3299.

23. A. Aballe, M. Bethencourt, F.J. Botana, M. Marcos, *Electrochemistry Communications* 1 (1999) 266-270.
24. A. Aballe, M. Bethencourt, F.J. Botana, M. Marcos, *Electrochimica Acta* 44 (1999) 4805-4816.
25. E. García-Ochoa, F. Corvo. *Electrochemistry Communications* 12 (2010) 826–830
26. S.V. Muniandy, W.X. Chew, C.S. Kan. *Corrosion Science* 53 (2011) 188–200
27. Xia Dahai, Song Shizhe, Wang Jihui, Shi Jiangbo, Bi Huichao, Gao Zhiming, *Electrochemistry Communications*, 2012, 15(1): 88-92.
28. Xia Dahai, Song Shizhe, Gong Wenqi, Jiang Yuxuan, Gao Zhiming, Wang Jihui, *Journal of food engineering*, 2012, 113(1): 11-18.
29. Xia Dahai, Shi Jiangbo, Gong Wenqi, Zhou Rongji, Gao Zhiming, Wang Jihui, *Electrochemistry*, 2012, 80 (11): 907-912.
30. Sun Y, Zeng WD, Zhao YQ, Qi YL, Ma X, Han YF. *Comput Mater Sci* 2010;48:686–91.
31. Vapnik V. *Statistical Learning Theory*[M]. Wiley, New York,NY,1998.
32. Cortes C, Vapnik V. Support-vector networks[J].*Machine Learning*,1995,20:273-297.
33. Boser B, Guyon I, Vapnik V. A training algorithm for optimal margin classifiers[J].*ACM press: In Proceedings of the Fifth Annual Workshop on Computational Learning Theory*,1992.
34. A.M.Homborg, T.Tinga, X.Zhang, *Electrochimica Acta* 70(2012)199-209
35. Mansfeld, Z. Sun, et al. *Corrosion Science* 43(2) (2001): 341-352.
36. Smulko, J, K. Darowicki, et al. *Electrochimica Acta* 47(8) (2002): 1297-1303.
37. S.Girija, U.Kamachi Mudali, et al. *corrosion science*. 49(2007) 4051-4068
38. Takumi Haruna, Yasuyuki Morikawa,et al. *corrosion science*. 45(2003):2093-2104
39. Hong-Ying Li,, Ji-Dong Hu, *Materials and Design* 42 (2012) 192–197
40. Lin C J. *Neural computation*,2001,13(2);307-317
41. J. Shawe-Taylor, N. Cristianini, *Kernel Methods for Pattern Analysis*, Cambridge University Press, New York, 2004.